

Adjoint wave-equation velocity analysis

U. Albertin^{*+}, P. Sava⁺⁺, J. Etgen⁺, and M. Maharramov⁺

⁺BP EPTG, Houston, Texas, ⁺⁺Colorado School of Mines, Golden, Colorado

Summary

A methodology for velocity updating using one-way wavefield extrapolation is described. The method is based on iterative optimization of two different objective functions; one that minimizes an image difference, and a second that optimizes focusing in the offset-at-depth domain, or equivalently, gather flatness in the angle domain. Various aspects of the method are illustrated with a 4D data example exhibiting velocity changes due to compaction, and a 3D example from an area exhibiting strong carbonate layering.

Introduction

In the past several years, wavefield extrapolation migration has become a standard tool for depth imaging in complex areas. In contrast, velocity updating techniques for depth imaging still rely primarily on ray tracing. This dichotomy has prompted significant interest in extending wavefield extrapolation methods to update velocities as well. Not surprisingly, the development of these methods is now following a direction very similar to that followed by early ray-based tomography development.

Historically, development of ray-based tomography for depth imaging followed two separate paths. Early techniques used differences in traveltimes observed between modeled data and actual seismic data (Bishop et al, 1983) as the primary measure of model fitness. As imaging moved to more complex areas, however, it became more difficult to obtain reliable time differences on input data, and hence an alternative methodology based on residual moveout on migrated offset gathers was developed (Stork, 1992). Just as in the ray-based case, in wave-equation tomography two methodologies are emerging. The first is based on wavefield differences between forward modeled data and seismic data (Tarantola, 1984), referred to as waveform tomography. The second and more recent methodology is based on a residuals obtained from image differences, or residuals associated with migrated gathers. In the context of downward wavefield-extrapolation, these methods are referred to as wave-equation velocity analysis (Biondi and Sava, 1999, Sava and Biondi, 2004), or one-way waveform inversion (Shen et al, 2003).

Here we present examples of these latter techniques: obtaining velocity updates from image differences, and from information contained in migrated gathers. We first give a general description of the methodology, and then

proceed to give 4D and 3D synthetic and data examples to illustrate various aspects of the technique.

Velocity backprojection from wavefield differences

The general principle behind wave-equation velocity analysis is that a change in the velocity model will create a corresponding change in the image. If we are given a downward-continued migrated image $I_c(x, z, h)$ that is a function of space and downward-continued offset, then a slowness change $d\mathbf{c}$ in the model will produce a corresponding change $d\mathbf{I} = \mathbf{I} - I_c$ in the image. The goal in wave-equation velocity analysis is to minimize this difference in an optimization scheme that solves for the slowness perturbation. If we assume a linear relation between the image difference and the slowness perturbation, the relation between them can be written as

$$d\mathbf{I} = \frac{\partial \mathbf{I}}{\partial \mathbf{c}} d\mathbf{c} \equiv \mathbf{S} d\mathbf{c}, \quad (1)$$

where for simplicity we refer to \mathbf{S} as the scattering operator. Since the inverse to the scattering operator cannot be found in general, the solution of eqn. (1) is done iteratively in a least-squares sense. The image difference is treated as a residual, and an initial estimate $d\mathbf{c}^*$ of the slowness perturbation change is computed by taking the adjoint of the scattering operator and applying it to the image residual. This is then used to compute a new slowness update and residual using either a linear or nonlinear solver. Since the computation of $d\mathbf{c}^*$ is done by a direct application of the adjoint operator \mathbf{S}^* to the image difference, the method falls into a class of methods often referred to as adjoint methods. Application of the adjoint operator involves upward continuing the image difference and then correlating it with the downward-continued wavefield used in the initial migration. Careful cancellation of phases in this procedure leads to an approximate slowness update. More details concerning this procedure are given by Sava and Biondi (2004).

Backprojection of image differences using downward and upward continuation can be effective in recovering slowness perturbations, and is particularly applicable to areas where such image differences are directly available, such as a 4D workflow. Figure 1 below illustrates this for a simple elliptical velocity perturbation, where recovery of

Adjoint wave-equation velocity analysis

the velocity perturbation from an image difference of a set of flat reflectors is shown in Figure 1b. Figure 2 further illustrates this with a 4D data example from the Valhall field. Over a period of two years, six surveys were acquired in this area, and were imaged with wave-equation techniques in order to monitor depletion of the reservoir. Figure 2b is the image difference obtained by subtracting images from surveys one and six. Depletion of the reservoir over time causes a compaction that increases velocities in the reservoir, while unloading in the overburden just above the reservoir causes a decrease in velocity. This trend in velocities has been verified by inversion techniques based on observed time differences between seismic events (Pettersen et al, 2006). Use of wave-equation velocity analysis on the image difference revealed a similar trend, seen in Figure 2c, where red indicates an increase in velocity, while blue indicates a decrease. Resolution of the backprojection was to within interbed distances in this case, or about 60m. Such an analysis can be helpful in corroborating information obtained in a time-difference analysis of 4D data.

Velocity backprojection via image focusing

Outside of 4D it is typically not possible to obtain a direct image difference for backprojection. Hence a different residual wavefield and objective function must be used (Shen et al, 2003). In this case a method for determining a suitable residual wavefield can be found in Claerbout's survey-sinking principle, which states that downward-continued sources and receivers spatially coincide at zero time if the velocity model is correct. If the model is incorrect, energy will not focus. All remaining energy outside of focused energy can then be used as a measure of model fitness, and can be used as a residual wavefield for velocity backprojection (Albertin et al, 2006, Shen et al, 2003). The principle can be stated mathematically by assuming there exists an operator H that annihilates the correct image (i.e. removes all focused energy), but leaves unfocused energy untouched, so that $HI_c = 0$, but $HI \neq 0$. Multiplying eqn. (1) by H we obtain $HI = HSdc$, which no longer explicitly involves the correct image. We then solve for the slowness perturbation in the adjoint sense to give

$$dc^* = (HS)^* HI. \quad (2)$$

This equation gives a general principle for velocity backprojection in order to optimize focusing in the image.

Illustration of how optimal focusing leads to flat angle gathers is illustrated in Figure 1 below, and is a result of relation between image offset (i.e. offset-at-depth) and

angle through slant stacking. In Figure 1 a simple elliptical slowness anomaly is backprojected using eqn. (2). The gathers before the update reveal substantial energy that has not focused near zero offset. This reveals itself as 'tails' extending away from the focused energy at zero offset. In the angle domain after slant stack, this energy translates into complex residual moveout, which can be seen in the corresponding angle gather. Use of the unfocused energy in an iterative backprojection eventually removes it, after which energy is well focused, and image gathers are flat.

Many choices are possible for the operator that removes focused energy. Initial methods employed by Biondi and Sava (1999) use a scanning technique across scale perturbations of the background model. Spatial picking and compositing of the image perturbations then leads to a residual field that corresponds spatially to the model with the flattest gather. Shen et al (2003) use a different technique based on differential semblance, where each trace in the angle gather is subtracted from its neighbor. This is equivalent to multiplying by offset in the image-offset domain, since multiplication by offset and differentiation in angle are related by slant stacking. This produces an appropriate residual field since it removes focused energy at zero offset. Such a residual is minimized when gathers are flat, assuming that the waveform along the gather is not significantly distorted due to AVA or irregular illumination effects. The residual field we used for Figure 1 is similar to that obtained using differential semblance.

An example of our technique for velocity recovery of a more complex velocity perturbation is shown in Figure 3. This is an area exhibiting significant carbonate layering, and an interpretation of the layering had been done prior to our testing. We used the interpreted perturbation to generate synthetic data for a relatively sparse set of flat layers that was migrated with the background field, and the residual field was then backprojected to give the velocity perturbation in Figure 3b.

One of the attractive features of a wave-equation velocity analysis that optimizes focusing is that in principle it does not rely on picking of gathers. Once the method for removal of focused energy is determined, the updating procedure is largely automatic. In practice this raises the issue of what the proper preconditioning of gathers for the residual field should be, since in ray based tomography, significant preconditioning of gather picks is often necessary for a proper update. Our experience thus far indicates that wave-equation based velocity analysis will require similar if not more care. Fluctuations in reflectivity, irregular illumination, and severe nonlinearity can all cause the procedure to arrive at an incorrect solution., and

Adjoint wave-equation velocity analysis

overcoming these difficulties remains an open question for further research.

Summary

We have discussed general methodologies for wave-equation velocity analysis based on both image differencing and optimal focusing using one-way wavefield extrapolation. Results on synthetics and data indicate that the methods are effective for the recovery of complex velocity anomalies for both complex imaging and 4D applications.

Acknowledgements

The authors wish to thank BP's Exploration Production Technology Group for their support and permission to publish this work. We would also like to thank Laurent Sirgue, Sverre Brandsberg-Dahl, Ken Matson, Olav Barkved, and Ray Abma for useful conversations related to this work. Special thanks to Frederic Billette for his guidance, Ole Askim for help with the Valhall data, Bill Symes for several helpful discussions, and Leon Thomsen for the initial suggestion of the application of wave-equation velocity analysis to 4D.

References

Albertin, U., Sava, P., Etgen, J., and Maharramov, M., 2006, Differencing and focusing in wave-equation velocity

analysis, 64th Ann. Mtg. Europ. Assoc. Expl. Geophys., Expanded Abstracts.

Bishop, T., Bube, K., Cutler, R., Langan, R., Love, P., Resnick, J., Shuey, R., Spindler, D., and Wyld, H., 1985, Tomographic determination of velocity and depth in a laterally varying media, *Geophysics* **50**, p. 903-923

Biondi, B. and Sava, P., 1999, Wave-equation migration velocity analysis, 69th Ann. Internat. Mtg., Soc. Expl. Geophys., Expanded Abstracts.

Pettersen, S.H, Barkved, O. I. and Haller, N., 2006, Time-lapse seismic inversion of data from a compacting chalk reservoir, submitted to the 76th Ann. Internat. Mtg Soc. Expl. Geophys.

Sava, P., and Biondi, B., 2004, Wave-equation migration velocity analysis. I. Theory, *Geophysical Prospecting* **52**, 593-606

Shen, P., Stolk, C., and Symes, W., 2003, Automatic velocity analysis by differential semblance optimization, 73rd Ann. Internat. Mtg., Soc. Expl. Geophys., Expanded Abstracts.

Stork, C., 1988, Reflection tomography in the post-migrated domain, *Geophysics* **57**, p. 680-692

Tarantola, A., 1984, Inversion of seismic reflection data in the acoustic approximation, *Geophysics* **49**, p. 1259-1266

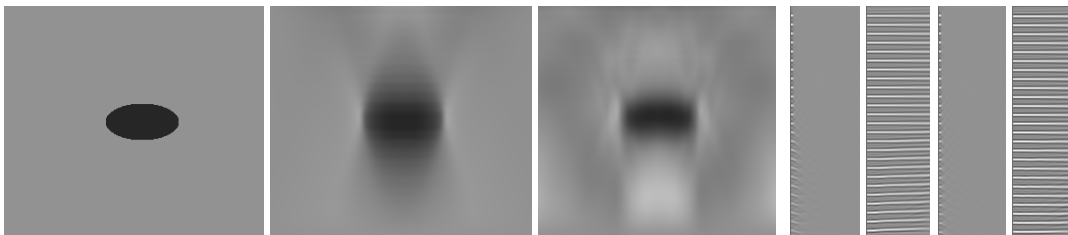


Figure 1: Sharp velocity anomaly backprojection. Figure 1a (left) shows an elliptical slowness anomaly. The model extent is about 500m horizontal by 250m vertical, with a background velocity of 2000m/s. Figure 1b (left center) shows the result of an image-difference backprojection with a 1% anomaly. Figure 1c (right center) shows the backprojection from image gathers for a 10% anomaly. Figure 1d (right, four gathers) shows a comparison of gathers near the left edge of the anomaly before and after the update. Gather 1 (left) is the image-offset gather, exhibiting tails due to improper focusing. Gather 2 is the corresponding angle gather with complex moveout. Gather 3 is the image-offset gather after the update, indicating the energy is now well focused. Gather 4 is the corresponding angle gather, which is now flat.

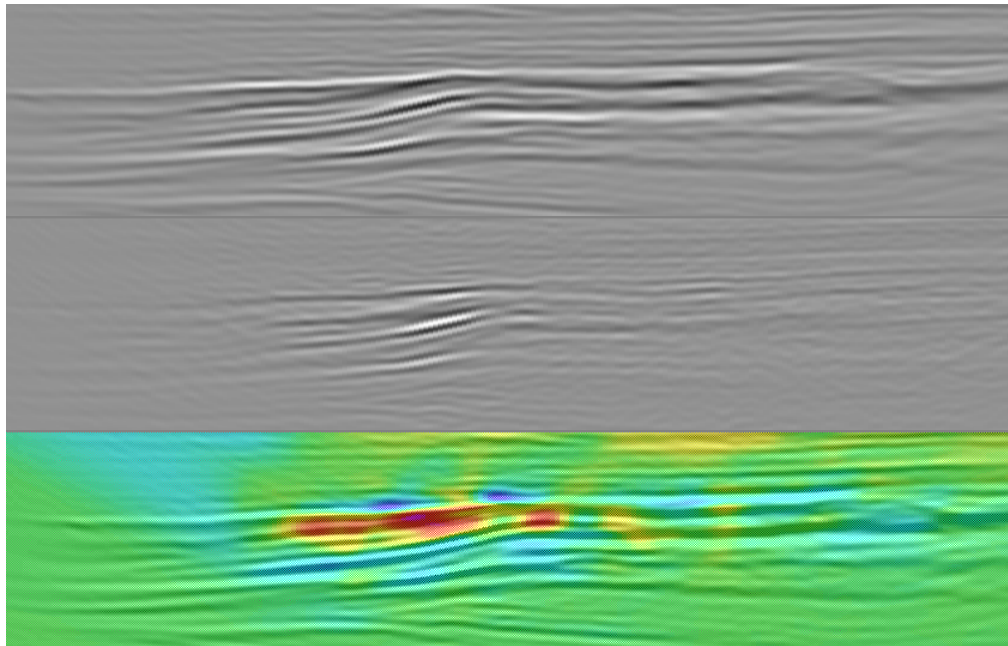


Figure 2: 4D wave-equation velocity backprojection from an image difference. Figure 2a (top) shows a section from the second of two 4D seismic sections in an area where reservoir depletion has occurred over time. Figure 2b (middle) shows the direct image difference obtained by subtracting the two 4D images data sets. Figure 2c (bottom) shows an overlay of the velocity backprojection of the difference in Figure 2b. This section begins at a depth of about 2300m, and has an extent of about 1100 m.

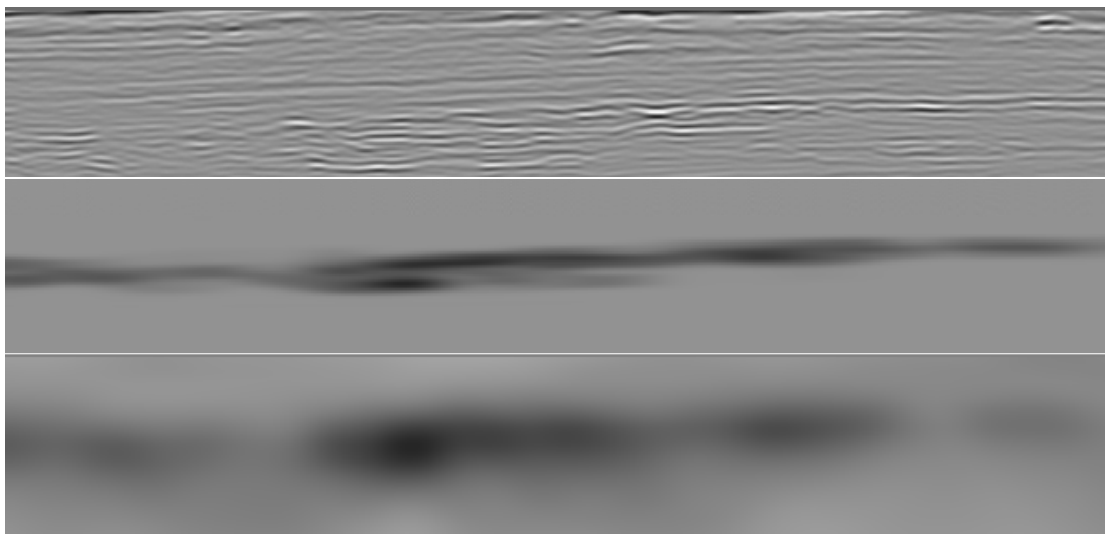


Figure 3 3D prestack wave-equation velocity backprojection from image gathers. Figure 3a (top) shows a section with significant anhydrite layering. Figure 3b (middle) is an interpretation of the slowness perturbation associated with the anhydrites, which represents about a 10 percent variation from the background. Figure 3c (bottom) is a 3D prestack backprojection from synthetic data and migrated image gathers using the perturbation in 3b. The vertical extent of this window is about 1200m at a depth of about 3000m, with maximum offset 3000m. Vertical resolution of the backprojection was about 300m in this case.

EDITED REFERENCES

Note: This reference list is a copy-edited version of the reference list submitted by the author. Reference lists for the 2006 SEG Technical Program Expanded Abstracts have been copy edited so that references provided with the online metadata for each paper will achieve a high degree of linking to cited sources that appear on the Web.

REFERENCES

- Albertin, U., P. Sava, J. Etgen, and M. Maharramov, 2006, Differencing and focusing in wave-equation velocity analysis: 64th Annual Conference and Exhibition, EAGE, Extended Abstracts.
- Biondi, B. and Sava, P., 1999, Wave-equation migration velocity analysis: 69th Annual International Meeting, SEG, Expanded Abstracts, 1723–1726.
- Bishop, T., K. Bube, R. Cutler, R. Langan, P. Love, J. Resnick, R. Shuey, D. Spindler, and H. Wyld, 1985, Tomographic determination of velocity and depth in a laterally varying media: *Geophysics* **50**, 903–923.
- Petterson, S. H., O. I. Barkved, and N. Haller, 2006, Timelapse seismic inversion of data from a compacting chalk reservoir: Presented at the 76th Annual International Meeting, SEG.
- Sava, P., and B. Biondi, 2004, Wave-equation migration velocity analysis, I, Theory: *Geophysical Prospecting*, **52**, 593–606.
- Shen, P., C. Stolk, and W. Symes, 2003, Automatic velocity analysis by differential semblance optimization: 73rd Annual International Meeting, SEG, Expanded Abstracts, 893–896.
- Stork, C., 1988, Reflection tomography in the postmigrated domain: *Geophysics* **57**, 680–692.
- Tarantola, A., 1984, Inversion of seismic reflection data in the acoustic approximation: *Geophysics* **49**, 1259–1266.